*Mathematical Geology, Vol. 38, No. 3, April 2006 (© 2006)*
DOI: 10.1007/s11004-005-9016-6

# Simultaneous Integration of Pressure, Water Cut, 1 and 4-D Seismic Data In Geostatistical Reservoir Modeling[1]

**Xian-Huan Wen,[2] Seong Lee,[2] and Tina Yu[2]**

*A geostatistically-based inverse technique, the sequential-self calibration (SSC) method, is used to update reservoir models so that they match observed pressure, water cut and time-lapse water saturation derived from 4-D seismic. Within the SSC, a steady-state genetic algorithm (GA) is applied to search the optimal master point locations, as well as the associated optimal permeability perturbations at the master locations. GA provides significant flexibility for SSC to parameterize master point locations, as well as to integrate different types of dynamic data because it does not require sensitivity coefficients. We show that the coupled SSC/GA method is very robust. Integrating dynamic data can significantly improve the characterization of reservoir heterogeneity with reduced uncertainty. Particularly, it can efficiently identify important large-scale spatial variation patterns (e.g., well connectivity, near well averages, high flow channels and low flow barriers) embedded in the reservoir heterogeneity. Using dynamic data, however, could be difficult to reproduce the permeability values on the cell-by-cell basis for the entire model. This reveals the important evidence that dynamic data carry information about large-scale spatial variation features, while they may be not sufficient to resolve the individual local values for the entire model. Through multiple realization analysis, the large-scale spatial features carried by the dynamic data can be extracted and represented by the ensemble mean model. Furthermore, the region informed by the dynamic data can be identified as the area with significant reduced variances in the ensemble variance model. Within this region, the cell-by-cell correlation between the true and updated permeability values can be significantly improved by integrating the dynamic data.*

**KEY WORDS:** history match; sequential-self calibration; genetic algorithm; production data integration; information of production data.

## INTRODUCTION

Dynamic data are the time dependent measurements of flow responses that are related to the reservoir properties through the flow equations, such as pressure, flow rate, fractional flow rate, saturation or 4-D seismic data. Various kind of dynamic data are usually available for most reservoirs under production. Integration

[1]Received 8 June 2004; accepted 8 July 2005; Published online: 27 May 2006.
[2]Chevron Energy Technology Company, 6001 Bollinger Canyon Rd., San Ramon, CA 94583, U.S.A.; e-mail: xwen@chevron.com

of dynamic data in reservoir model requires that the solutions of flow equations based on the reservoir model are in reasonable agreement with actual measurement of those data. Traditionally, this integration is done through a history match procedure. In current industry practice, history matching is commonly performed manually on a reservoir model via repeated flow simulations and local or regional multipliers to reservoir properties are frequently used. By adjusting regions and the associated multipliers, a history match could be achieved using either trial-and-error or other more advanced methods (e.g. Milliken and Emanuel, 1998). These techniques usually create artificial boundaries (discontinuities) inside the reservoir, and potentially destroy the correlation relationship and other geological features built into the initial geostatistical reservoir model. Thus, the prediction power of such history matched models may be limited.

A more sophisticated approach is to integrate the dynamic data during the reservoir modeling stage, i.e., dynamic data are directly used when constructing geostatistical reservoir model via geostatistically-based inversion techniques. Integration of dynamic data in geostatistical reservoir model is an important and yet outstanding challenge during the reservoir modeling. A great deal of effort has been devoted to develop new techniques for such purpose (e.g., Caers and others, 2002; Hu, 2000; Landa, 2001; Landa and Horne, 1997; Oliver, He, and Reynolds, 1996; Reynolds, He, and Oliver, 1999; Wen, Deutsch, and Cullick, 1998a,b; Wen, Yu, and Lee, 2004). These techniques provide methods of preconstraining geostatistical reservoir model before they go to the traditional manual history match phase. This minimizes the most time consuming and costly part of a history match process. A review of these inverse techniques can be founded in Yeh (1986) and Wen, Deutsch, and Cullick (1997). Most geostatistically-based inversion methods attempt to match production data by modifying the initial model in such a way that it preserves the underlying geostatistical features built into the initial model, such as histogram, variogram, and other soft constraints (e.g., Landa, 2001; Vasco, Yoon, and Datta-Gupta, 1998; Wang and Kovscek, 2000; Wen, Deutsch, and Cullick, 1998a,b). Others directly incorporate an optimization process within the geostatistical framework to generate reservoir models that match dynamic data (e.g., Hu, 2000; Caers and others, 2002). Typically, an inverse technique is needed for such integration, in which flow equations must be solved many times within a nonlinear optimization procedure (Sun, 1994; Tarantola, 1987). Both finite difference and streamline flow modeling can be used for the dynamic data integration. Streamline-based inverse techniques have shown great potential due to the straightforward delineation of flow regions of each well pair and the fast calculation of sensitivity coefficients (e.g. Agarwal and Blunt, 2003; Caers and others, 2002; Cheng and others, 2004; Milliken and Emanuel, 1998; Vasco, Yoon, and Datta-Gupta, 1998; Wen, Deutsch, and Cullick, 1998b, 2003).

The Sequential Self-Calibration (SSC) method is very efficient and robust for integrating dynamic data in geostatistical reservoir models (Gomez-Hernandez,

Sahuquillo, and Capilla, 1997; Capilla, Gomez-Hernandez, and Sahuquillo, 1997; Wen, 1996; Wen, Deutsch, and Cullick, 1998a,b). The SSC uses an optimization process to modify/update the original reservoir model to match dynamic data preserving geostatistical features in the original model. The efficiency of the SSC method comes from the master point concept and global updating. The master points are employed to reduce the number of parameters. Perturbations at the master points are then propagated into entire model to achieve the global updating. Current implementation of the SSC method can use either a gradient-based optimization or genetic algorithm (GA) to compute optimal perturbation values at the master point locations (Wen, Yu, and Lee, 2004).

Gradient-based optimization requires the calculation of sensitivity coefficients that measure the changes of reservoir flow responses with respect to the change of reservoir properties. In practice, the sensitivity calculations comprise the most central processing unit (CPU) time in the inversion. A great deal of effort has been dedicated to speed up this calculation, particularly via streamline simulation (e.g., Vasco, Yoon, and Datta-Gupta, 1998; Wen, Deutsch, and Cullick, 1998a,b, 2003). A number of new approaches have also been presented along this line, including the generalized travel time method (Wu and Datta-Gupta, 2002; Cheng and others, 2004). However, the sensitivities are usually not accurately computed which causes difficulty in optimization. Also, gradient-based optimizations are often trapped by local minimums for highly nonlinear problems. On the other hand, GA does not need sensitivities, and it attempts to search for global minimum. It is thus easier to implement for different type of parameters, as well as for complex reservoir models. The major drawback of GA is that it requires more flow simulation runs to evaluate the model fitness than gradient-based methods. Nevertheless, GA brings significant flexibility for SSC. Under the SSC framework, both master point locations and values of reservoir properties at the master points can be considered as variables in GA.

Previously, SSC has been applied to integrate production dynamic data including pressure, water cut, and water saturation data (Wen, Deutsch, and Cullick, 2002; Wen, Yu, and Lee, 2004). 4-D seismic (time-lapse 3-D seismic) has shown to be able to predict fluid saturation changes in the reservoir by recording the acoustic responses at different times due to the change of fluid impedance (Wang and Nur, 1988). Typically, the difference between the two 3-D seismic data sets recorded at different times is an indicator of the areas in the reservoir where the distribution of fluids has changed. Due to the close relationship between the 4-D seismic and reservoir dynamic data, we can also consider 4-D seismic as part of dynamic production data (Huang, Meister, and Workman, 1997; Kretz, Le Ravalec-Dupin, and Roggero, 2004).

In this study, we use GA as an optimization method in the SSC to find the optimal master point locations and the associated optimal changes of reservoir permeability at the master point locations. We also include the saturation changes

interpreted from time lapse seismic, together with pressure and water cut at wells as our dynamic data. This represents a very comprehensive integration of all available dynamic data. Using the coupled SSC/GA, multiple realizations of reservoir model could be updated, all of which match the dynamic data. This allows for assessing the uncertainty reduction of reservoir characterization due to the integration of dynamic data. By analyzing the multiple updated realizations, we can further reveal the spatial variation features that are common to all realizations, and can be considered as the essential information carried by the given dynamic data.

This paper is organized as follows. We first briefly review the framework of the coupled SSC/GA method. We then present the results with a synthetic reservoir model using the coupled SSC/GA inversion. The results are further analyzed and discussed in more details before drawing conclusions.

## THE COUPLED SSC/GA METHOD

Using geostatistical methods, we can construct multiple realizations of reservoir model that are conditioned to all available static data. Our goal is to modify these models (referred as initial models) so that the flow solutions computed from the modified models (referred as updated models) match the observed dynamic data. In addition, we wish that the updated models preserved the geostatistical features (e.g., histogram, variogram, as well as other soft constraints) in the initial models. In this study, we only update permeability model to minimize the following objective function:

$$O = \sum_{w_p=1}^{n_{wp}} W_p \left[\hat{p}(w_p) - p(w_p)\right]^2 + \sum_{w_f=1}^{n_{wf}} \sum_{t_f=1}^{n_{tf}} W_f [\hat{f}(w_f, t_f) - f(w_f, t_f)]^2 + \sum_{i=1}^{n_s} W_s \left[\delta\hat{s}(i) - \delta s(i)\right]^2 \quad (1)$$

where $\hat{p}(w_p)$ and $p(w_p)$ are the observed and simulated pressure at well $w_p$. $\hat{f}(w_f, t_f)$ and $f(w_f, t_f)$ are the observed and simulated water cuts at well $w_f$ at time $t_f$. $\delta\hat{s}(i)$ and $\delta s(i)$ are the observed and simulated water saturation changes at cell $i$ interpreted from time lapse seismic data. $W_p$, $W_f$, and $W_s$ are the weights assigned to pressure, water cut, and water saturation changes. $n_{wp}$ and $n_{wf}$ are the number of wells that have pressure and water cut data. $n_{tf}$ is the number of time steps for water cut data. And $n_s$ is the number of cells with water saturation data available.

The sequential-self calibration (SSC) method allows for fast updating of initial reservoir models to match dynamic flow data (Gomez-Hernandez, Sahuquillo, and Capilla, 1997; Capilla, Gomez-Hernandez, and Sahuquillo, 1997). The unique features of the SSC algorithm include (1) the concept of *master point* that reduces

the parameter space to be estimated in optimization, (2) the propagation procedure through *kriging* that accounts for spatial correlation of perturbations. Originally, SSC uses a gradient-based optimization method and iteratively modifies the initial reservoir models to match the dynamic data. It requires the iteration to self-correct the linear assumption used during the optimization, as well as the inaccurate sensitivity coefficients. Typically, less than 20 iterations are required in a 2-D setting. Previous SSC results revealed that the final updated models are usually smoother than the initial models due to the successive addition of smooth kriged perturbation fields at each iteration (Wen, Deutsch, and Cullick, 2002).

Recently, a steady-state genetic algorithm (DeJong, 1975) has been incorporated into the SSC as an alternative optimization method to find the optimal master locations and the associated optimal changes at those locations (Wen, Yu, and Lee, 2004). Using GA, only one global updating is needed and the smoothing effect by adding a smooth perturbation field is also reduced to the minimum. Within the steady-state GA, the selection method is the traditional roulette wheel (fitness proportionate) selection. In this method, the probability of an individual to be chosen equals to the fitness of the individual divided by the sum of the finesses of all individuals in the population. The fitness is evaluated through the objective function (Eq. (1)) computed from the flow simulation results. Two genetic operators are used to generate offspring: uniform crossover and Gaussian mutation. Uniform crossover picks gene values from two parents randomly to compose the offspring. Gaussian mutation changes a gene value to a new value based on a Gaussian distribution around the original value.

The main steps of the coupled SSC/GA can be summarized as follows (Wen, Yu, and Lee, 2004):

1. Construct initial realizations: Multiple equal-probable initial property realizations are created by conventional geostatistical methods using specific histogram and variogram consistent with the data. If static (hard and soft) data are available, they should be honored with conditional simulation. Each realization is processed one at a time with the following steps.
2. Solve the flow equations for the current model using specific boundary and well conditions to obtain simulation responses.
3. Compute the objective function that measures the mismatch between the observed dynamic data and the flow solutions. If the objective function is smaller than a preselected tolerance, this realization is considered to honor the dynamic data and we move to the next realization. Otherwise, proceed to the following steps.
4. Choose the number of master points and solve an optimization problem via GA to find the optimal master point locations and the associated perturbations of reservoir property at these locations.

5. Propagate the perturbations at master locations through the entire field by kriging the computed perturbations at master points. The model is then globally updated by adding the smooth kriged perturbation field to the initial model. Note that this propagation process is embedded in the internal GA process, rather than performed at the end of GA.

Application of the SSC method requires a variogram model that defines the way of spreading of perturbations from the master points to the entire model. The resulting multiple equal-probable realizations provide assessment of uncertainty of reservoir model and then can be translated into uncertainty of flow predictions for reservoir management. It is noted that only one global updating is added to the initial model at the end of the above process where GA is used to search for such updating via iteration.

In GA, we first select a fixed number of master points and generate an initial population of initial master point locations and the associated permeability values at these locations. The number of master points depends on the correlation length of the model. We employ 1–3 master points per correlation length in each direction. The master point locations are selected with the stratified random method (i.e., random within a regular coarse grid that covers the entire model). Other methods of selecting master point locations (e.g., fix location and purely random methods) may be used as well. In previous studies, the stratified random method has yielded the best results due to its flexibility and overall field coverage (Wen, Yu, and Lee, 2004).

The log-permeability values at the master points are initially generated from a Gaussian function with the mean and variance consistent with the model and with the constraints of the minimum and maximum values. Note that if the $\ln(k)$ model is not Gaussian, we can use a different distribution function. Also if we know the conditional pdf of each location from soft static data, we can use such pdf to generate initial $\ln(k)$ values. This provides significant flexibility to honor different kind of constraints for the geostatistical model.

Based on the generated $\ln(k)$ values at master point locations, as well as those at the initial model, we can compute the perturbations at the master point locations by subtracting the values at the initial model from the generated values. We then interpolate the perturbation values at non-master point locations using kriging. An updated model is computed by adding the interpolated perturbation field to the initial model. The fitness of each model is evaluated by its objective function after flow is solved for the model.

With $Nm$ master points, the GA genome is an array of $Nm$ integer for master point locations and $Nm$ real numbers for their associated $\ln(k)$. The steady-state GA is then used to search for the new master point locations and the associated permeability values until the mismatch between the flow simulation results and observed historical production data is minimized. We retain the best individual

(the optimal master point locations and the associated $\ln(k)$ values) at the end of the GA. The GA has 60% overlapping, i.e., at each generation, the better half of the population remains while the worse half is replaced by newly created offspring. New offspring always make into population, regardless of whether or not their fitness are better than the worse half of the original population.

## AN EXAMPLE

In this section, we demonstrate the applications of the coupled SSC/GA method for constructing reservoir permeability models from pressure, water cut and time lapse water saturation data using a synthetic data set. In the example, we assume porosity is known and constant as $\phi = 0.2$.

### Reference Field and Dynamic Data

Figure 1(A) shows a 2-D geostatistical reference field ($50 \times 50$ grid with cell size 80 feet $\times$ 80 feet). The model is generated using the Sequential Gaussian Simulation method (Deutsch and Journel, 1998). The $\ln(k)$ has Gaussian histogram with mean and variance of 6.0 and 3.0, respectively. The unit of permeability ($k$) is milli Darcy (1 Darcy $= 9.8697 \times 10^{-13}$ m$^2$). The variogram is spherical with range of 800 feet and 160 feet in the direction of 45° and 135°, respectively. We assume a water injection well (I) at the center of the model with four production wells (P1 to P4) at the four corners. The injection rate at the injection well (I) is 1600 STB/day and the production rate for the four production wells is 400 STB/day/well. The thickness of the reservoir is constant of 100 feet. All four boundaries have no-flow boundary conditions. The initial pressure is constant at 3000 psi (1 psi $= 6894.757$ Pa) for the entire field. The main features of

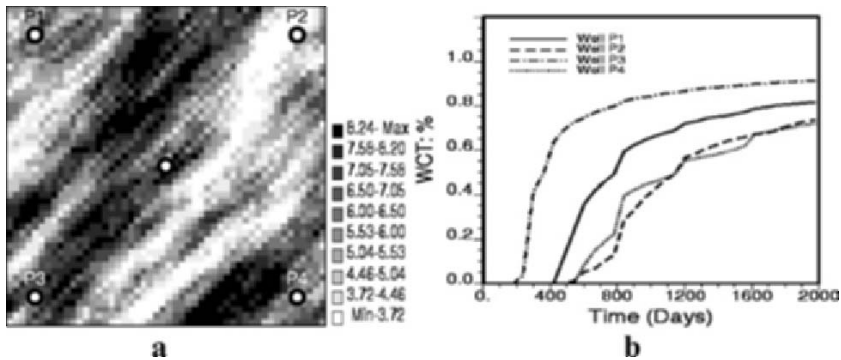


**Figure 1.** (a) The reference $\ln(k)$ field. (b) Water cuts from the four production wells.

this field are: (1) a high permeability zone and a low permeability zone in the middle of the field, (2) high interconnectivity between well I and well P3, (3) low interconnectivity between well I and wells P2 and P4. This reference field is considered as the true model, and our goal is to reconstruct reservoir models, based on some dynamic data and geostatistics, that are as close to this true field as possible.

The reservoir is initially saturated with oil. Mobility ratio of oil and water is 10 and standard quadratic relative permeability curves are used with zero residual saturation for oil and water. Compressibility and capillary pressure are ignored. Water injection and production are solved using a streamline simulator for 2000 days. Pressure field is updated every 400 days to account for the change of mobility during the streamline simulation. We assume the observed dynamic data are: (1) bottom hole pressure (BHP) of each well at the end of the simulation, (2) water cut history of each production well, and (3) time lapse water saturation distribution at 400 and 800 days. The "observed" BHP for I and P1–P4 are given in Table 1, the water cuts of four production wells are shown in Figure 1(B). Note that the fast water breakthrough at well P3 and late breakthrough at wells P2 and P4. Water saturation distributions at 400 and 800 days are given in Figures 2(A, B). The difference of water saturation between the two times is given in Figure 2(C). Considering the fact that 4-D seismic data usually can not provide very accurate water saturation data, we use the binary value as our time-lapse water saturation data. If the saturation different between the two times is greater than 0.1 at a given cell, this cell is marked as a cell with saturation change. Otherwise, no change of saturation is observed. Figure 2(D) shows the binary map with black being the cells that experience saturation changes and white with no saturation changes. This binary map is considered as the 4-D seismic data used in the objective function calculation as the observed saturation changes. This is similar to Kretz, Le Ravalec-Dupin, and Roggero (2004) who used gas-flow indicator to represent the presence/absence of gas interpreted from 4-D seismic. Note that the methodology presented in this paper can also use the actual values of saturation change, as well as the associated uncertainty (accuracy) in the saturation data as 4-D seismic data as well. The use of binary map represents a very uncertain 4-D seismic data.

**Table 1.** Comparison of BHPs from the Two Initial and Updated Models with the Reference Field

| Well name | I | P1 | P2 | P3 | P4 |
|---|---|---|---|---|---|
| Reference | 3043 | 2985 | 2468 | 3022 | 2917 |
| Initial, #1 | 3135 | 2489 | 2920 | 2995 | 2974 |
| Updated, #1 | 3108 | 2991 | 2551 | 3008 | 2919 |
| Initial, #2 | 3037 | 3007 | 3022 | 2925 | 2872 |
| Updated, #2 | 3050 | 2949 | 2500 | 3032 | 2929 |

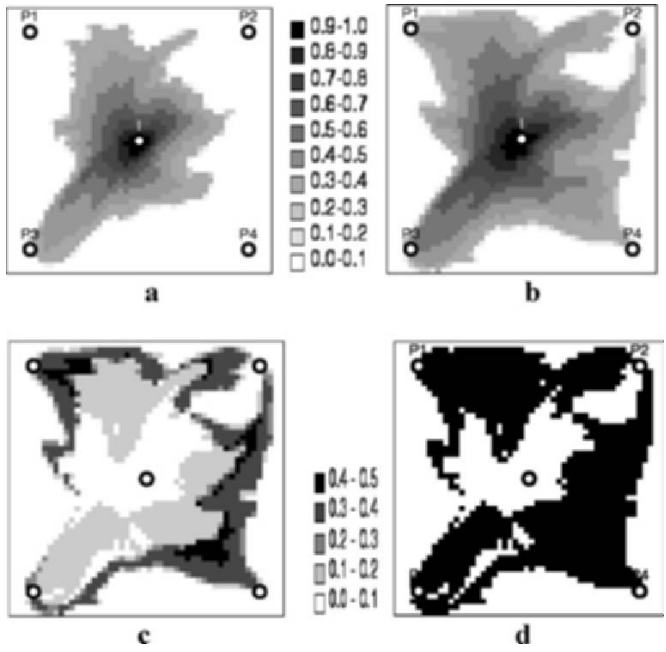


**Figure 2.** Water saturation distribution from the reference field: (a) water saturation at 400 days; (b) water saturation at 800 days; (c) changes of water saturation from 400 to 800 days; (d) binary map of saturation changes (black: with saturation change; white: no saturation change).

It should also be noted that a more sophistical way of integrating 4-D seismic data may be through the direct matching of forward modeled seismic responses (e.g., amplitude) with 4-D seismic data. This, however, involves the complicated forward seismic-wave-propagation modeling that requires information about densities and compressional velocities for reservoir fluids and rocks, as well as reservoir porosity, pressure and fluid saturations. In this paper, we have simplified the 4-D seismic data by representing them as binary time-lapse water saturation changes. It could be reasonably expected, under the conditions considered in this paper, that 4-D seismic responses might be matched as long as the spatial variations of reservoir properties (e.g., permeability), as well as reservoir pressure and water saturation are matched. Another important issue on the 4-D seismic data is the scale difference between the seismic data and model cell size. Usually, 4-D seismic data inform about a scale larger than the scale of geostatistical (or flow simulation) model, particularly for vertical scale. Such difference can be taken into account using the coupled SSC/GA, we have, however, ignored such difference in this study.

## Update Models with SSC/GA

We now present results of two individual realizations using the coupled SSC/GA method. We first generate multiple initial realizations using the same histogram and variogram as the reference field. Neither well data nor other soft data are used while generating the initial models. It should be noted, however, that some hard (e.g., core data) or soft (e.g., seismic data) data are usually available in most practices. All relevant data should be used while constructing the initial models and these constraints can be preserved using the SSC. We do not account for these data due to the concern of scale issue in practical situations (i.e., the available data are usually at scales different from the cell size used in simulation).

We use 25 master points and they are selected stratified randomly within each of the $5 \times 5$ coarse grid blocks (each coarse block consists of $10 \times 10$ fine cells). The population size used in GA is 50 with 50 generations evolved. The crossover rate is 90%, mutation rate is 1% and replacement rate is 60%. The weights used in the objective function (Eq. (1)) are $W_{\mathrm{p}} = 20$, $W_{\mathrm{f}} = 2$ and $W_{\mathrm{s}} = 1$. These weights are chosen so that the different components in the objective function have similar magnitude. With each initial model as a starting model, GA searches for the optimal locations of 25 master points and the associated optimal changes of permeability values at those locations. The optimal changes at master points are then propagated to the entire model using kriging to create a smooth global perturbation field. This perturbation field is added to the initial model resulting in the updated model that matches the dynamic data. The best individual at the last generation is chosen as the final updated model. Note that all 50 models (i.e. the whole population) at the last generation could be considered as updated models since they are all very close in terms of matching the dynamic data. We choose the best individual for each initial model to better represent the uncertainty space in the initial and updated models. Figure 3 shows two initial permeability fields (top row) and the resulting perturbation fields (middle row) together with the master point locations (plus) obtained by the SSC/GA. The final updated models are shown at the bottom row of Figure 3. The BHPs at wells computed from the initial and updated models are given in Table 1. The matches of water cut and water saturation changes for the initial and updated models are given in Figures 4 and 5.

Compared to the reference field (Fig. 1(A)), it is clear that the spatial variation patterns in the two initial models are quite different from the reference model (Fig. 3, top row). In initial model 1, although wells I and P2 are not directly connected by high permeability, they are indirectly connected by the two high permeability stripes adjacent to them. Also, the wells I and P3 are not well connected enough. For the initial model 2, both the high connectivity between wells I and P3, and the low connectivity between wells I and P2 are not represented. After inversion, the updated models display spatial variation features very similar to the reference model (Fig. 3, bottom row). Particularly, in both models, in order

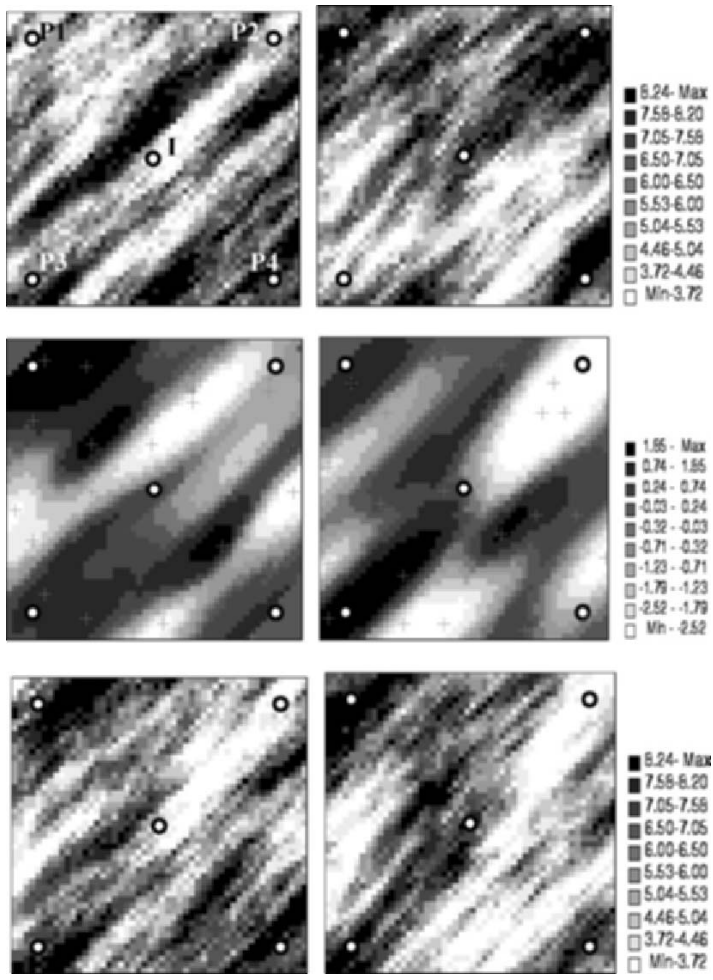


**Figure 3.** Two initial realizations of ln(k) model (*top*), the computed perturbation fields and master point locations (*middle*), and the resulting updated models (*bottom*). Left is for model 1 and right for model 2.

to match the production data, permeabilities in the region between wells I and P3 are increased, while in the region between wells I and P2, permeabilities are reduced (see Fig. 3).

Flow responses from the initial models are significantly deviated from the "observed" data (see Table 1 and Figs. 4 and 5). Well pressure is mainly affected by the permeabilities around the given well. We can see that BHP at well P1 is significantly smaller than the observed one in the initial model 1 due to the smaller

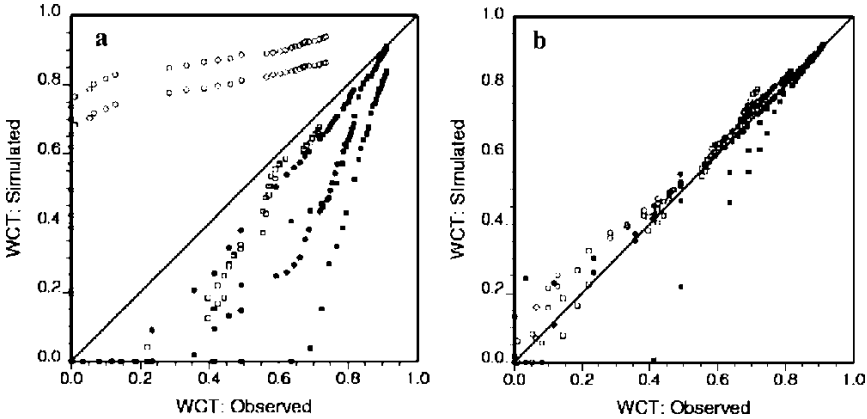


**Figure 4.** Scatter plots of water cuts from the two initial and updated models with respect to the observed data (i.e., results from the reference field): (a) initial models; (b) updated models. Filled circle for P1, open circles for P2, filled squares for P3, and open squares for P4.

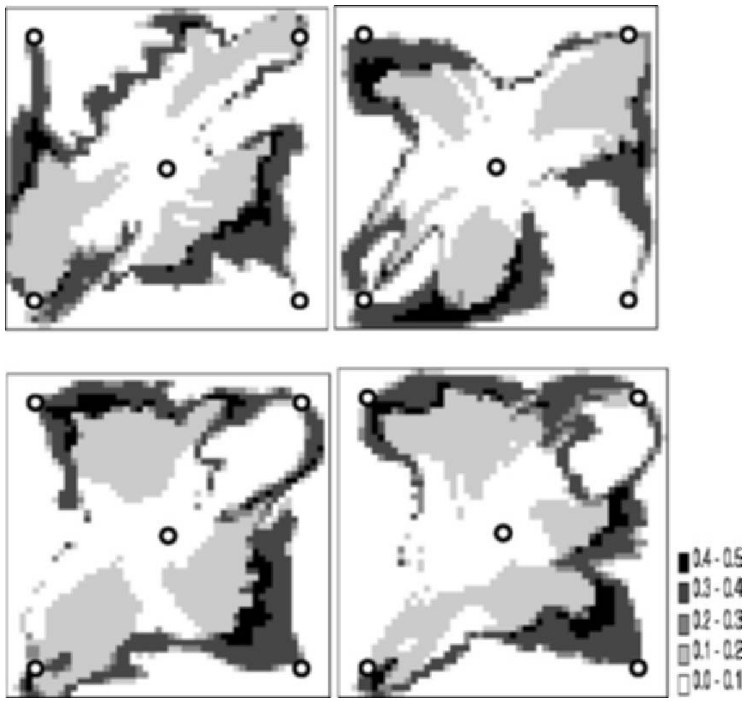


**Figure 5.** Water saturation changes from the two initial (*top row*) and updated (*bottom row*) models.

permeabilities around this well for this model (see Table 1 and Fig. 3). Pressures at well P2 are dramatically overestimated in the both initial models due to higher permeabilities around the well than in the reference field. The BHPs from the updated models are close to the observed data.

Water cuts at a given producer are primarily determined by the spatial connectivity between the injector and the producer. In both of the initial models, too higher water cuts are observed for well P2 (open circles in Fig. 4(A)) compared to the true model which is caused by the high spatial connectivity between wells I and P2 in the initial models. In comparisons, because of the lack of strong high permeability connection between the wells I and P3, water cuts at well P3 (filled squares in Fig. 4(A)) are underestimated in the two initial models. After inversion, all water cut data are closely matched as shown in Figure 4(B).

Saturation distribution data reveal more detailed spatial variation features for the entire reservoir model. They are the combined effects of the complex spatial features, well patterns and boundary conditions. From Figure 5, we can see that the spatial features for the changes of water saturation in the initial models (top row) are very different from the reference field shown in Figure 2. After updating (Fig. 5, bottom row), they display spatial features much closer to the reference field.

## Uncertainty Analysis

From above results, it is demonstrated that the SSC/GA is able to update reservoir models to match the "observed" dynamic data. One of the advantages of using SSC is that we can update multiple equally-likely initial realizations to match the same dynamic data to assess uncertainty reduction in the reservoir characterization due to the integration of dynamic data. This is similar to the randomized maximum likelihood method as presented by Liu, Betancourt, and Oliver (2001). Using multiple realization analysis, we can also extract some essential common spatial features among all updated models. These common spatial features could be considered as the real reservoir information carried by the matched dynamic data.

We update 100 initial models using SSC/GA and present the ensemble results of the all updated realizations by the ensemble mean and variance in Figure 6. The ensemble mean field (i.e. the E-type estimation) represents the common features displayed in the multiple realizations with the variance field indicating the associated variation (uncertainty) among these realizations. Note that the ensemble mean and variance fields for the 100 initial models should be close to constants of 6.0 and 3.0 since no conditioning data are used when generating the initial model. From Figure 6, we can see that, by incorporating dynamic data, the large-scale variation patterns in the reference model is very well captured with reduced uncertainty. More specifically, the mean field closely reproduces (a) the permeability

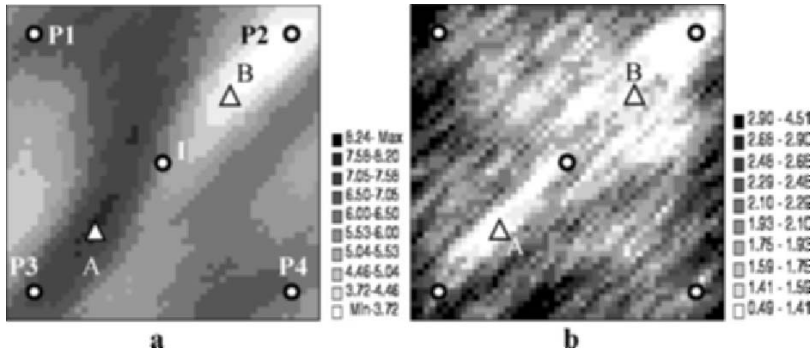


**Figure 6.** Ensemble results of ln($k$) from 100 updated models: (a) mean field; (b) variance field.

values around the wells, (b) the high permeability connection between wells I and P3, and between wells I and P1, as well as (c) the low permeability connection between wells I and P2. The uncertainties in these areas are small indicating that these important features are present in realizations with high probability.

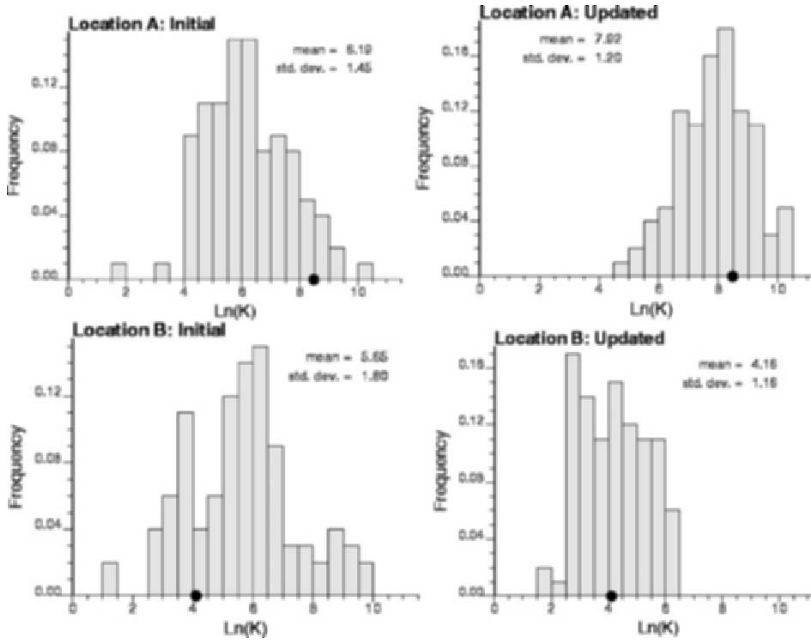


**Figure 7.** Histograms of ln($k$) values at locations A and B from the 100 initial and updated realizations. The bullets are the true values from the reference field.

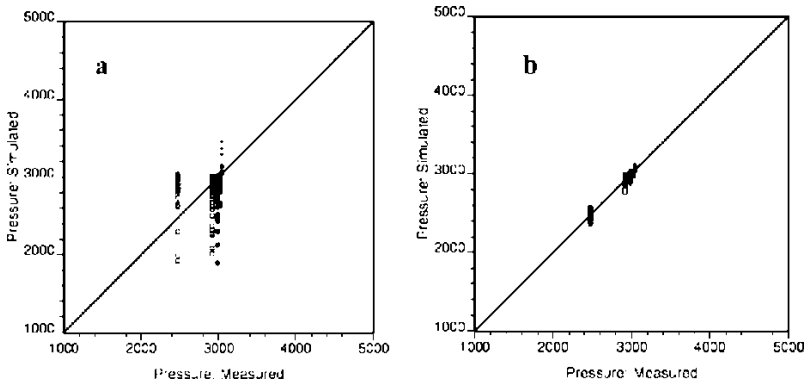


**Figure 8.** Match of BHPs at five wells: (a) initial models; (b) updated models.

More specifically, Figure 7 shows the histograms of ln($k$) values at two selected locations (A and B in Fig. 6(A)) from the 100 initial and updated realizations. For the initial realizations, ln($k$) mean value at location A is too low compared to the true value, while it is too high at location B. The variations/uncertainties at both locations are large (i.e., large variances). After updated by SSC/GA, the uncertainties (variance) are significantly reduced with the means of both histograms being very close to the true values.

The above results demonstrate that dynamic production data carry important information on the spatial variations of reservoir properties in the geological model. Integration of such dynamic data can significantly improve the characterization of reservoir model and reduce the model uncertainty.

The matches of pressure, water cut and saturation from the 100 initial and updated models are presented in Figures 8–10. The BHPs at the five wells vary drastically within the 100 initial models. After inversion, the computed BHPs are very close to the data (see Fig. 8). Water cut curves from the initial models are neither accurate (significantly deviate from the reference field) nor precise (with large uncertainty/spreading, see Fig. 9(A)). Particularly, water breakthroughs at well P2 are too fast for almost all models, while most of them are too slow for wells P1 and P3. After inversion, the water cuts are very closely reproduced in all updated models (see Fig. 9(B)).

Figure 10 shows the ensemble (mean and variance) of water saturation changes computed from the 100 initial and updated models. As expected, the mean saturation change from the initial models does not display any specific patterns, except 45° elongation consistent with the permeability variogram anisotropy with large uncertainty (Fig. 10, top row). The ensemble saturation changes from the updated models display spatial patterns very similar to the result of the reference

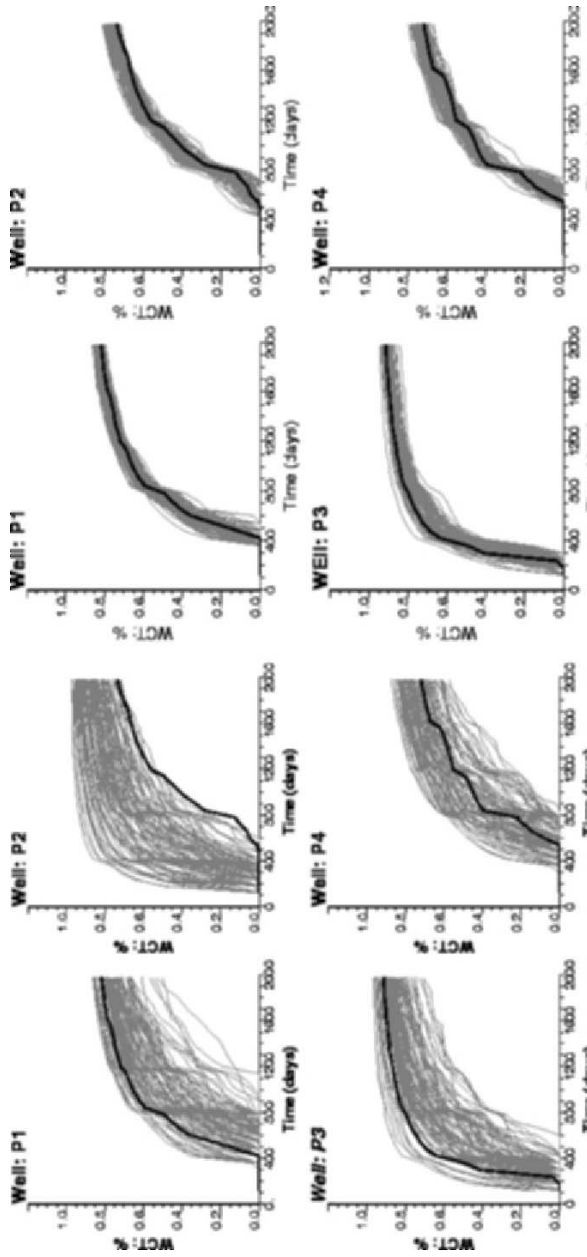


**Figure 9.** Match of water cut data: (a) 100 initial models; (b) 100 updated models. *Thick solid lines* are the water cuts from the reference field.

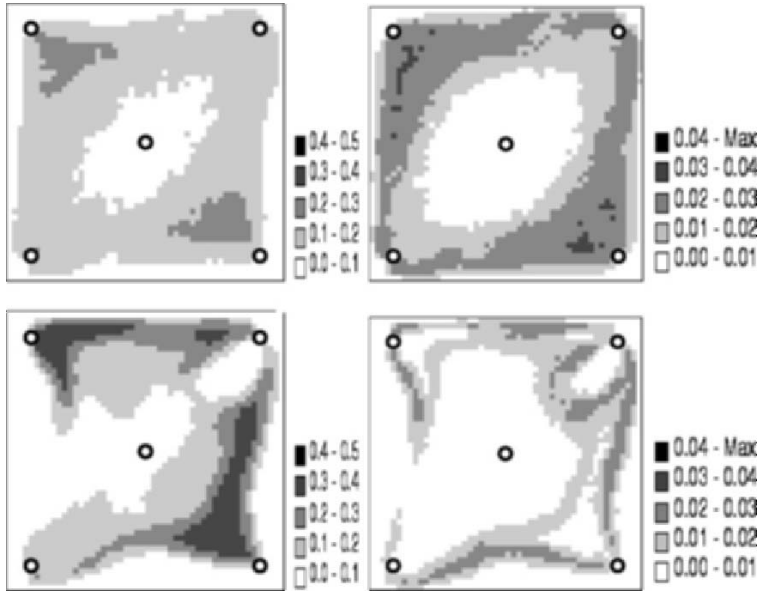


**Figure 10.** Ensemble results (*left*: mean and *right*: variance) of water saturation changes from 100 initial (*top*) and updated (*bottom*) models.

field with significantly reduced variance /uncertainty (see Fig. 2 and bottom row of Fig. 10).

The histograms of different components in objective function from the 100 initial and updated models are given in Figure 11. The values of objective function from the initial models display significantly larger variation with much larger means compared to those from the updated models. Note that the objective functions for saturation changes are reduced by about half. It clearly indicates the difficulty of matching data on the cell by cell basis.

## DISCUSSION

Based on visual inspections of Figures 1 and 3, it is clear that the spatial variation patterns in the updated models are very close to the reference field while the initial models display significantly different patterns. To further analyze the results, we plot the cell to cell scatter plots of the two initial and updated models with respect to the reference field as shown in Figure 12. From this figure, we note that there is almost no correlation between the initial and reference models (left column of Fig. 12), which is as expected since they are realizations independent of the reference field. The correlation between the updated and reference models

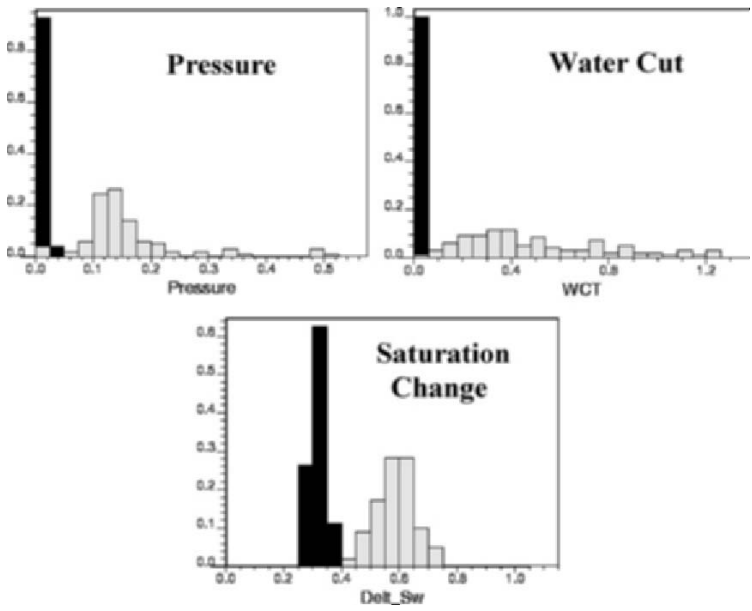


**Figure 11.** Histograms of different components in the objective function computed from the initial (*gray*) and updated (*black*) models.

is somewhat improved, but surprisingly still very weak for both models even although the spatial patterns displayed in the updated models are quite close to the reference model. This reveals very important evidence that the information on reservoir heterogeneity carried by dynamic data is in terms of spatial variation patterns rather than individual point values. For example, the water cut data mainly reflect the degree of spatial connectivity between the injector and producer, while well pressure is primarily affected by the averaged permeability values around the well regions. Saturation changes are determined by more complex spatial features in the reservoir model that interact with flow at different times. The spatial patterns reflected by the dynamic data, although visually recognizable, are usually on scales larger than cell size and may be very complex and difficult to quantify using simple and single point statistics. Pattern recognition techniques or multiple point statistics may be useful to compare these spatial variation patterns.

To further prove this observation, we present the scatter plots of permeability values at master point locations from the 100 initial and updated models with respect to the values at the same locations from the reference field (see Fig. 13). Again, as expected, no correlation is observed for the initial model. Correlation for the updated model, although improved, is also weak indicating the poor

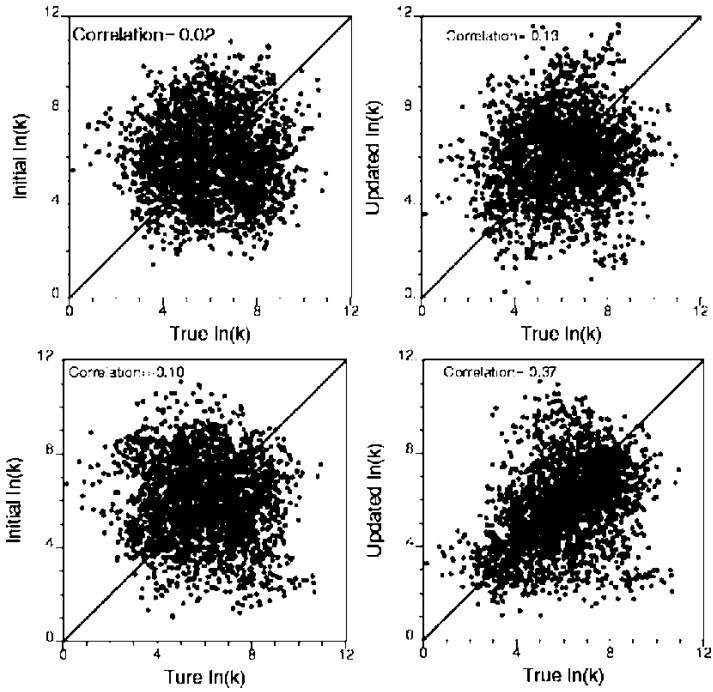


**Figure 12.** Cell by cell scatter plots of the two initial and updated models with respect to the reference model: left for initial; right for updated; top for model 1; and bottom for model 2.

reproduction of the true permeability values on the cell-by-cell basis for the entire model.

Based on above analysis, it is evident that dynamic data reflect the large-scale complex spatial variation features (patterns) embedded in the reservoir model, rather than the individual local cell values. By integrating such dynamic data, we can efficiently identify and reproduce these large-scale spatial features, whereas, it is very difficult (if not impossible) to resolve the individual local cell values. This provides an explanation on why, during the history match process, it is not very critical to match the local details as long as the large-scale features are in place. These large-scale features are the essential spatial variation patterns carried by the dynamic data, which can be extracted from multiple realizations and represented in terms of the ensemble mean field (see Fig. 6(A)). This ensemble mean field represents the common features among different realizations that are critical for matching the dynamic data. Note that the complex large-scale features are displayed in this figure.

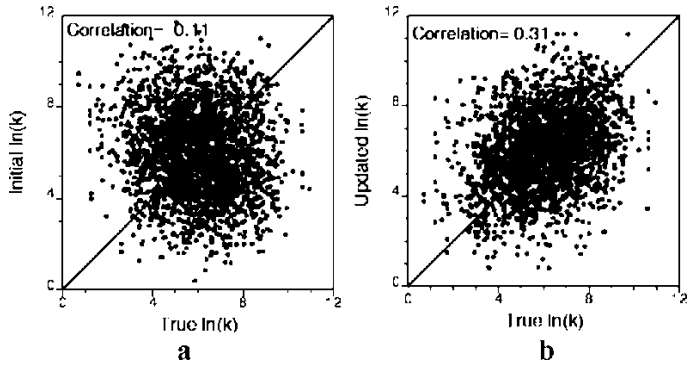


**Figure 13.** Scatter plots of the ln($k$) values at master point locations from the 100 initial and updated models with respect to the reference model: (a) initial; (b) updated.

Figure 14 shows the scatter plots of ensemble mean models of initial and updated realizations with respect to the reference model. For the initial model, the ensemble mean model has no feature with almost constant value of 6, while the updated mean model displays significantly larger variations than the initial model that are much more correlated to the reference model.

Finally, it is reasonable to believe that dynamic data can only reveal spatial heterogeneity information for the areas within which the permeability distribution can significantly influence the dynamic data. We refer this area to be the region informed by the dynamic data, which can be identified from the ensemble variance model (Fig. 6(B)). The weak point-to-point correlation between the updated model and the reference model observed above may also be due to the high uncertainty

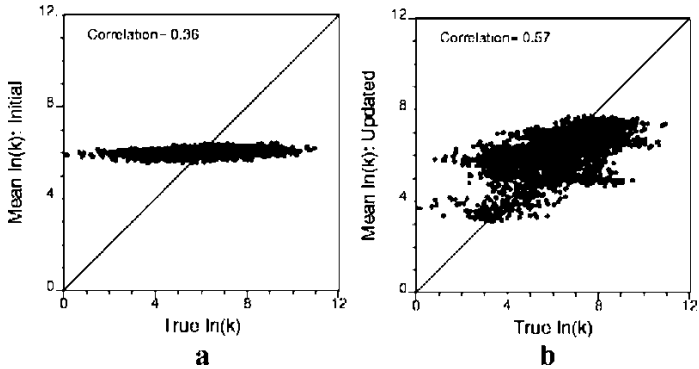


**Figure 14.** Scatter plots of the ln($k$) values for the mean initial and updated models with respect to the reference model: (a) initial; (b) updated.

in the updated model at some regions that do not have significant impact on the dynamic data. To further illustrate the value of integrating dynamic data, we identify the region informed by the dynamic data to be the subregion where the ensemble variance is reduced to less than half of the initial value (i.e., $<1.5$ for our example, see Fig. 15(F)). This subregion is consistent with the interwell areas with two major spatial features that are revealed by the mean model (i.e., the high and low permeability zones, see also Figs., 1(A) and 6(A)). We then plot the scatter plots of permeability values within this region from the same two initial and updated models as in Figure 12 with respect to the values at the same locations from the reference field (see Fig. 15(A)–(D)). The scatter plot of updated ensemble mean values within the same region with respect to the reference model is given in Figure 15(E). Compared to Figures 12 and 14 where all cells are plotted and the improvement of correlation for the updated models are not significant, we now see the drastic improvement of correlation for the updated models (Figs. 15(B), (D), (E)) over the initial models (Fig. 15(A), (C)). From this analysis, we demonstrate that dynamic data could not only reveal important spatial features, but also better reproduce the local permeability distribution within the area informed by the dynamic data.

## CONCLUSIONS

We use the coupled SSC/GA to update multiple realizations of geostatistical reservoir model that simultaneously match pressure, water cut, and saturation changes interpreted from 4-D seismic data. Through a synthetic example, it is shown that the coupled SSC/GA is very flexible and robust to integrate different types of dynamic data. Results from this paper show that, by integrating dynamic data, reservoir heterogeneity can be better characterized resulting in models that are significantly closer to the real model in terms of the spatial variation patterns with much less uncertainty.

We also show that dynamic data are mainly controlled/influenced by some large-scale spatial features within the influence region. These features may be different for different types of dynamic data. In other words, the resolution of dynamic data is primarily limited to large-scale features. It is not sufficient to resolve individual local cell values from the entire model using dynamic data. To match the particular dynamic data, it is not necessary to use the actual values at particular cells as long as the spatial features essentially controlling the dynamic data are captured (e.g., well connectivity, averaged values around wells, flow channels, or flow barriers). Thus, individual cell values may still subject to large uncertainty even though a large number of dynamic data are used, particularly in the areas not influenced by the dynamic data. Through multiple realization analysis, we can effectively identify the complex large-scale features/patterns that impact the dynamic data by extracting the common features among all realizations

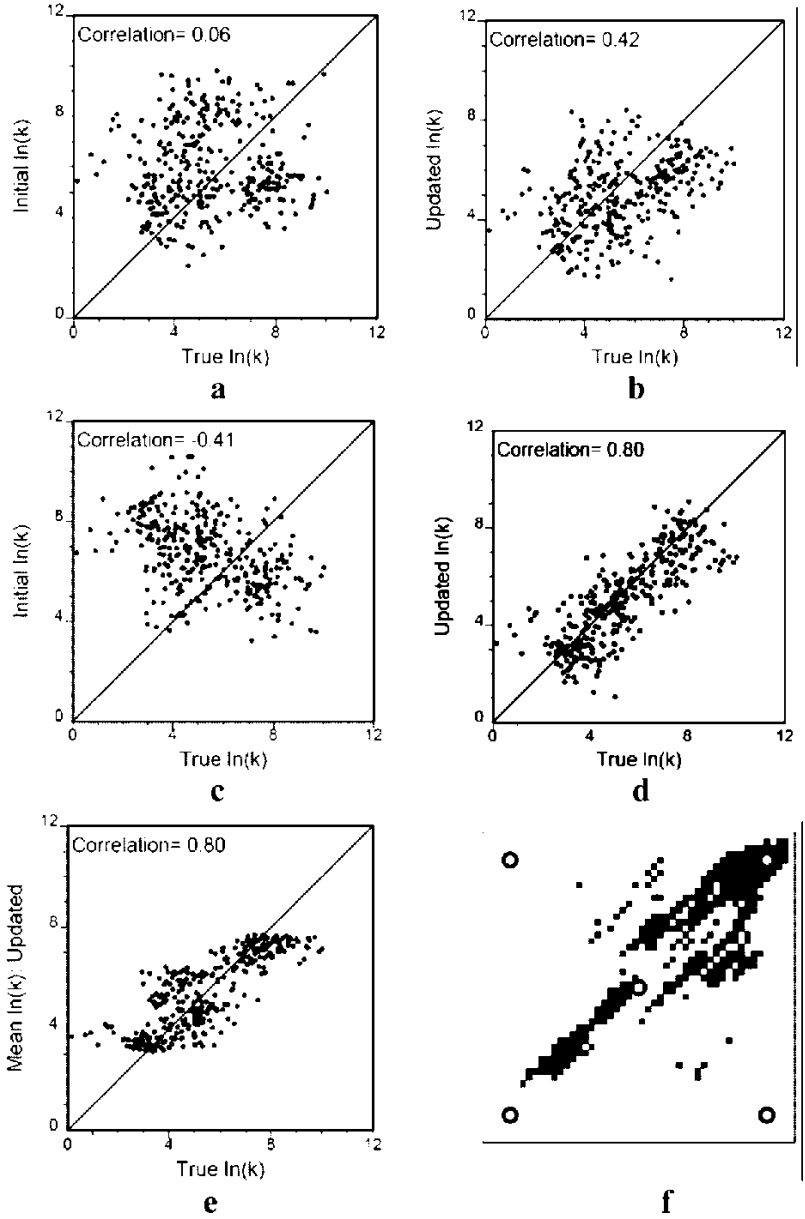


**Figure 15.** Scatter plots of ln($k$) values within the area informed by the dynamic data for the initial, updated and mean models with respect to the reference model: (a) initial model 1; (b) updated model 1; (c) initial model 2; (d) updated model 2: (e) updated mean model; (f) region informed by the dynamic data with ensemble variance less than 1.5 (*in black*).

(i.e., by computing the mean, or E-type, model). On the other hand, by analyzing the ensemble variance model, we can identify the area informed by the production data. We show that within the area informed by the dynamic data, significant improvement could be achieved to reproduce the local permeability values. Thus, the traditional way of evaluating the quality of inversion parameter models based on cell-to-cell value comparison should apply only to the values within the area informed by the dynamic data.

On the other hand, since dynamic data are not sensitive to individual local values, it would not be very efficient to use the individual cell permeability as parameters in any inverse formulation. A better way of parameterization is to use some parameters that can create global or large-scale pattern changes, such as the master point concept in the SSC formulation. This provides another explanation to why SSC is so efficient on matching dynamic data compared to other geostatistically-based inverse methods that use single point parameters.

Finally, it should be noted that we just use saturation changes to represent the time-lapse seismic data. This may oversimplify the 4-D seismic integration. The more sophistical way of integrating 4-D seismic data requires the direct matching of forward modeled seismic responses (e.g., amplitude) with data. Nevertheless, we might reasonably expect, under the conditions considered in this paper, that 4-D seismic responses through forward modeling could be matched as long as the spatial variations of reservoir properties (e.g., permeability), as well as reservoir pressure and water saturation are matched. The same framework presented in this paper can be applied to directly match the forward modeled 4-D seismic, as well as to account for the data inaccuracy and scale difference in 4-D seismic data.

## REFERENCES

Agarwal, A., and Blunt, M. J., 2003, Streamline-based method with full-physics forward simulation for history-matching performance data of a North Sea field: Soc. Petrol. Engr. J., v. 8, no. 2, p. 171–180.

Caers, J., Krinshnan, S. Wang, Y., and Kovscek, A. R., 2002, A geostatistical approach to streamline-based history matching: Soc. Petrol. Eng. J., v. 7, no. 3, p. 250–260.

Capilla, J. E., Gomez-Hernandez, J. J., and Sahuquillo, A., 1997, Stochastic simulation of transmissivity fields conditional to both transmissivity and piezometric data, 2. Demonstration on a synthetic case: J. Hydrol., v. 203, no. 1–4, p. 175–188.

Cheng, H. Wen, X.-H. Milliken, W. J., and Datta-Gupta, A., 2004, Field experiences with assisted and automatic history matching using streamline models: Soc. Petrol. Eng. paper 89857, SPE Annual Technical Conference and Exhibition, Houston, TX, Sept. 26–29, 2004.

DeJong, K. A., 1975, An analysis of the behavior of a class of genetic adaptive systems: Ph.D. Thesis, University of Michigan, 260 p.

Deutsch, C. V., and Journel, A. G., 1998, GSLIB: Geostatistical software library and user's guide, 2nd ed: Oxford University Press, New York, 369 p.

Gomez-Hernandez, J. J., Sahuquillo, A., and Capilla, J. E., 1997, Stochastic simulation of transmissivity fields conditional to both transmissivity and piezometric data, 1. The theory: J. Hydrol., v. 203, no. (1–4), p. 162–174.

Huang, X., Meister, L., and Workman, R., 1997, Reservoir characterization by integration of time-lapse seismic and production data: Soc. Petrol. Eng. paper 38695, SPE Annual Technical Conference and Exhibition, San Antonio, TX, Oct. 5–8, 1997.

Kretz, V., Le Ravalec-Dupin, M., and Roggero, F., 2004, An integrated reservoir characterization study matching production data and 4D seismic: Soc. Petrol. Eng. Eval. Eng., v. 7, no. 2, p. 116–122.

Landa, J. L., and Horne, R. N., 1997, A procedure to integrate well test data, reservoir performance history and 4-D seismic information into a reservoir description: Soc. Petrol. Eng. paper 38563 presented at the SPE Annual Technical Conference and Exhibition, San Antonio, TX, October 5–8, 1997.

Landa, J. L., 2001, Technique to integrate production and static data in a self-consistent way: Soc. Petrol. Eng. paper 71597 presented at the SPE Annual Technical Conference and Exhibition, New Orleans, 30 September–3 October, 2001.

Hu, L. Y., 2000, Gradual deformation and iterative calibration of Gaussian-related stochastic models: Math. Geol., v. 32, no. 1, p. 87–108.

Liu, N., Betancourt, S., and Oliver, D. S., 2001, Assessment of uncertainty assessment methods: Soc. Petrol. Eng. paper 71624 presented at SPE Annual Technical Conference and Exhibition, New Orleans, 30 September–3 October, 2001.

Milliken, W. J., and Emanuel, A., 1998, History matching finite difference models with 3D streamlines: Soc. Petrol. Eng. paper 49000 presented at the SPE Annual Technical Conference and Exhibition, New Orleans, 27–30 September, 1998.

Oliver, D. S., He, N., and Reynolds, A. C., 1996, Conditioning permeability fields to pressure data, *in* Proceedings of the 1996 European Conference for the Mathematics of Oil Recovery, Leoben, Austria, 3–6 September, 1996, p. 1–11.

Reynolds, A. C., He, N., and Oliver, D. S., 1999, Reducing uncertainty in geostatistical description with well testing pressure data, *in* Schatzinger R. A. and Jordan J. F., eds., Reservoir characterization-recent adv.: American Association of Petroleum Geologists, Tulsa, 149–162 p.

Sun, N.-Z., 1994, Inverse problem in groundwater modeling: Kluwer Academic Publishers, Boston, 337 p.

Tarantola, H., 1987, Inverse problem theory: Methods for data fitting and model parameter estimation: Elsevier, Amsterdam, 613 p.

Vasco, D. W., Yoon, S., and Datta-Gupta, A. 1998, Integrating dynamic data into high-resolution reservoir models using streamline-based analytical sensitivity coefficients: Soc. Petrol. Eng. paper 49002 presented at the SPE Annual Technical Conference and Exhibition, New Orleans, LA, Sept. 27–30, 1998.

Wang, Y., and Kovscek, A. R., 2000, A Streamline approach to history matching production data: Soc. Petrol. Eng. paper 59370 presented at the SPE/DOE symposium on Improved Oil Recovery, Tulsa, OK, April 3–5, 2000.

Wang, Z., and Nur, A., 1988, Effect of temperature on wave velocities in sands and sandstones with heavy hydrocarbones: Soc. Petrol. Eng. Reservoir Eng., p. 158–164.

Wen, X.-H.,1996, Stochastic simulation of groundwater flow and mass transport in heterogeneous aquifers: Conditioning and problem of scales: Ph.D. Thesis, Technical University of Valencia, Valencia, Spain., 260 p.

Wen, X.-H., Deutsch, C. V., and. Cullick, A. S., 1997, A review of current approaches to integrate flow production data in geological modeling, *in* Report 10, Stanford Center for Reservoir Forecasting, Stanford, California.

Wen, X.-H., Deutsch, C. V., and Cullick, A. S., 1998a, High resolution reservoir models integrating multiple-well production data: Soc. Petrol. Eng. J., p. 344–355.

Wen, X.-H., Deutsch, C. V., and Cullick, A. S., 1998b, Integrating pressure and fractional flow data in reservoir modeling with fast streamline-based inverse method: Soc. Petrol. Eng. paper number

48971, presented at the SPE Annual Technical Conference and Exhibition, New Orleans, LA, Sept. 27–30, 1998.

Wen, X. H., Deutsch, C. V., and Cullick, A. S.,2002, Construction of geostatistical aquifer models integrating dynamic flow and tracer data using inverse technique: J. Hydrol., v. 255, p. 151–168.

Wen, X.-H., Tran, T. T., Behrens, R. A., and Gomez-Hernandez, J. J., 2002, Production data integration in sand/shale reservoirs using sequential self-calibration and geomorphing: A comparison: Soc. Petrol. Eng. Reservoir Eval. Eng., p. 255–265.

Wen, X. H., Deutsch, C. V., and Cullick, A. S., 2003, Inversion of dynamic production data for permeability: Fast streamline-based computation of sensitivity coefficients of fractional flow rate: J. Hydrol., v. 281, no. 4, p. 296–312.

Wen, X. H., Yu, T., and Lee, S., 2004, Coupling sequential-self calibration and genetic algorithms to integrate production data in geostatistical reservoir modeling: Paper presented at 7th International Geostatistical Congress, Banff, Canada.

Wu, Z., and Datta-Gupta, A., 2002, Rapid history matching using a generalized travel time inversion method: Soc. Petrol. Eng. J., v. 7, no. 2, p. 113–122.

Yeh, W. W.-G., 1986, Review of parameter identification procedure in groundwater hydrology: The inverse problem: Water Resour. Res., v. 22, no. 2, p. 85–92.